Journal of Power Sources 195 (2010) 6225–6231

Contents lists available at ScienceDirect

Journal of Power Sources

journal homepage: www.elsevier.com/locate/jpowsour

Plastic dye-sensitized photo-supercapacitor using electrophoretic deposition and compression methods

Hsin-Wei Chen[a], Chih-Yu Hsu[a], Jian-Ging Chen[a], Kun-Mu Lee[b], Chun-Chieh Wang[a], Kuan-Chieh Huang[a], Kuo-Chuan Ho[a,c,*]

[a] Department of Chemical Engineering, National Taiwan University, Taipei 10617, Taiwan
[b] Photovoltaics Technology Center, Industrial Technology Research Institute, Hsinchu 31040, Taiwan
[c] Institute of Polymer Science and Engineering, National Taiwan University, Taipei 10617, Taiwan

ARTICLE INFO

Article history:
Received 9 October 2009
Received in revised form
23 December 2009
Accepted 6 January 2010
Available online 13 January 2010

Keywords:
Compression method
Dye-sensitized solar cell (DSSC)
Electrophoretic deposition (EPD)
PEDOT film
Photo-supercapacitor

ABSTRACT

A plastic photo-rechargeable capacitor is studied using a three-electrode configuration, separating a flexible dye-sensitized solar cell (DSSC) and a supercapacitor by sharing a common Pt electrode. The thick and uniform TiO_2 film is formed by using commercially available TiO_2 nanocrystals, which are treated in an isopropyl alcohol without surfactant by the electrophoretic deposition (EPD) to deposit the mesoporous TiO_2 photoanode film with good adherence onto the plastic substrate. Afterward, a static mechanical compression technique as the post-treatment is employed to the electrophoretic deposited film in order to enhance the particles connection. In addition, a supercapacitor using PEDOT (poly(3,4-ethylenedioxythiophene)), which is potentiostatically electropolymerized to form a thick film, is fabricated to store the energy. The flexible DSSC part is fabricated with a TiO_2 film of 10.9 μm thickness and it can provide photoelectric conversion efficiency up to 4.37% under 1 sun illumination. The photocapacitor is made with such a flexible DSSC and a supercapacitor with *ca.* 0.5 mm thick PEDOT film, which provides a specific capacitance of 0.52 F cm^{-2}.

1. Introduction

In the past decade, the dye-sensitized solar cells (DSSCs) have attracted significant attention and interest in research due to the simple processes, materials, and equipments that can reach low-cost mass production and the superior light-to-electricity conversion efficiency (~11%) [1], which is a cheap alternative way to the conventional silicon solar cells [2–4]. Moreover, by employing dye purification procedure or using other new heteroleptic polypyridyl ruthenium complex dyes with high molar extinction coefficients, Grätzel group even achieved a strikingly high efficiency over 11% [5,6]. The traditional DSSCs are consisted of dye-sensitized nanocrystalline TiO_2 photoanode on the transparent conductive oxide (TCO) layer such as F-doped SnO_2 layered glasses (FTO glasses), electrolyte with iodide/tri-iodide redox couple and Pt-counter electrode. For the TiO_2 photoanode fabricated on the FTO glass substrate, it has the shortages of expensiveness, fragility and rigidity that make the glass-based DSSC less likely to be mass produced.

Therefore, plastic-based flexible DSSCs have caught much attention for the light-weight, flexibility of shape and potential to mass production. However, for the fabrication process of the TiO_2 photoanode on ITO-PET (ITO on poly(ethylene terephthalate)) or ITO-PEN (ITO on poly(ethylene naphthalate)), temperature must be controlled below 150 °C. Thus, due to the low-temperature limitation on the photoanode, the plastic-based DSSCs have several challenges to be overcome. The TiO_2 electrodes to be assembled in the conventional glass-based DSSCs are usually annealed at 450–500 °C to achieve acceptable adhesion to the glass substrate with great interparticle connection, which is a crucial challenge for plastic-based DSSCs. Besides, porosity must be preserved in the TiO_2 photoanode after any post-treatment that used in the plastic-based DSSCs.

In order to prepare good interconnection and adherent TiO_2 photoanode in plastic-based DSSCs, some known methods can be applied both to the TiO_2 paste and the TiO_2 film. For example, binder-free TiO_2 paste was modified by adding some weak base (such as ammonia) into the acidic TiO_2 colloids that enable low-temperature chemical sintering to reach photovoltaic power conversion efficiency (η) up to 3.52% at 1 sun [7]. Other binder-free nanocrystalline TiO_2 paste with good interparticle connection using low-temperature coating process and dye N712 achieved 5.8% efficiency at 1 sun [8,9]. Some unique procedures have been proposed to increase the interparticle connection and to

* Corresponding author at: Department of Chemical Engineering, National Taiwan University, Taipei 10617, Taiwan. Tel.: +886 2 2366 0739; fax: +886 2 2362 3040.
E-mail address: kcho@ntu.edu.tw (K.-C. Ho).

0378-7753/$ – see front matter © 2010 Elsevier B.V. All rights reserved.
doi:10.1016/j.jpowsour.2010.01.009

improve the cell efficiency. They included UV-sintering procedure [10], microwave-sintering process [11], ball milled TiO_2 slurries [12], and the hexafluorosalisilic acid addition to promote low-temperature connection of the TiO_2 nanoparticles [13]. Another approach to fabricate a well adherent TiO_2 photoanode other than doctor-blade method was based on the electrophoretic deposition (EPD) [14]. EPD has attracted significant attention recently for several advantages such as shorter deposition time, simple experimental process, applicability for deposition on some complicated shape substrate, controllable deposition film thickness, and no need for binder. A mesoporous nanocrystalline TiO_2 film prepared by EPD on ITO-PET with chemical post-treatment and thermal treatment to increase interparticles connections has demonstrated devices η of 4.1% under 100 mW cm^{-2} [14].

For the fabrication of plastic-based DSSCs the conventional high temperature (450–550 °C) sintering process cannot be applied, therefore chemical sintering, binder additives, and mechanical compression method are useful steps to increase the particles connection. Among them, the mechanical compression process is the most effective method in preparing the TiO_2 film from the viewpoints of easy process control and short processing time [15–17]. The TiO_2 film prepared by the EPD process on ITO-PET, based on isopropanol suspensions of commercial P25 titania nanoparticles with small amount of magnesium nitrate and 2% deionized water under mechanical compression at 200 bar, has achieved η value of 1.66% under 100 mW cm^{-2} [18]. Cathodic EPD of commercially available TiO_2 nanocrystals (P25 and P90, Degussa) on FTO coated glass substrates with mechanical compression and high temperature (450–550 °C) sintering processes has reached η value of 8.5% (100 mW cm^{-2}) [19] and further coating the nano-sized inorganic layer (MgO) on the TiO_2 film with only mechanical compression has achieved η value of 6.2% (100 mW cm^{-2}) [20]. Another method was done by transferring a TiO_2 composite film sintered at high temperature (450 °C) to a ITO-PET substrate by application of high pressure and reached η of 5.8% under 100 mW cm^{-2} [21]. Recently, the highest η value of 7.4% (100 mW cm^{-2}) has been achieved [22] with TiO_2 paste prepared by the hydrolysis of $Ti(OCH(CH_3)_2)_4$, followed by the autoclave treatment and applying doctor-blade and mechanical compression processes on the ITO-PEN plastic substrate.

Photocapacitor is a device combined with the capacitor and photovoltaic solar cell that can store the direct solar energy. However, the capacitor must be durable for repeated charging and discharging, which need a redox-free liquid electrolyte to achieve long lifetime, rapid response to current change and high charge–discharge durability performance. In the developments of photocapacitors, we chose a conducting polymer film PEDOT (poly(3,4-ethylenedioxythiophene)) with redox-free electrolyte for it has good conductivity, fast switching, low toxicity, mechanically flexible applicability and high specific capacitance approaching 5 F cm^{-2} as a good candidate for supercapacitor electrode materials [23]. Similar concept for such three-electrode type photocapacitor has been proposed by Miyasaka's group [24,25], who used carbon/carbon electrode in the capacitor. It is generally accepted that the three-electrode type photocapacitor offers advantages in rapid discharge performance, high charge/discharge durability and long lifetime. The photo-supercapacitor is a simple three-electrode sandwiched device consisting of a photoelectrode, an internal bifunctional Pt electrode working simultaneously as both cathode and anode, in junction with two electrolytes. For the fabrication of photo-supercapacitor, the DSSC part can be roll-to-roll produced along with sandwiching the supercapacitor simultaneously. Afterward, the photo-supercapacitor was sealed to form an integrated device. Once the photo-supercapacitor can be made continuously by the roll-to-roll process, it is possible that the cost of the integrated device can be lower than that of the separate devices.

In this work, the EPD method was employed to deposit mesoporous TiO_2 photoanode film onto the plastic substrate. Subsequently, the use of the compression method enhances the quality of the TiO_2 film. With the use of the prepared plastic photoelectrode, a photo-rechargeable supercapacitor was constructed using a PEDOT film with a three-electrode configuration, separating DSSC and supercapacitor parts by sharing a common Pt electrode. The PEDOT film was potentiostatically electropolymerized to form a thick film (*ca.* 0.5 mm) with a specific capacitance (0.52 F cm^{-2}). We optimized the photoelectrode after investigating the effects of the TiO_2 thickness and the compression pressure in order to enhance the photocharging performance. The improvement for the pressed TiO_2 photoanode was also confined by the plastic DSSC which gave the best photovoltaic parameters, including power conversion efficiency (η), short-circuit current density (J_{sc}) and fill factor (*FF*) of 4.4%, 8.4 mA cm^{-2} and 0.71, respectively, under 100 mW cm^{-2}.

2. Experimental

2.1. Materials

Lithium iodide (LiI) and iodine (I_2) were obtained from Merck; 4-tert-butylpyridine (TBP) and tert-butyl alcohol were obtained from Acros; ethanol, neutral cleaner and isopropyl alcohol (IPA) and the monomer 3,4-ethylenedioxythiophene (EDOT) were obtained from Aldrich. Acetonitrile (ACN), 3-methoxypropionitrile (MPN), tertiary butanol, $LiClO_4$ and LiI were also obtained from Merck and water molecules were removed by molecular sieves (4 Å).

2.2. Preparation of TiO_2 photoanode and photo-supercapacitor assembly

ITO-PEN (15 Ω sq.$^{-1}$, Peccell Technologies, Inc.) was used as the substrate for the TiO_2 photoanode. Commercial nanocrystalline TiO_2 particles (P25, 25 nm, 75% anatase and 25% rutile, Degussa) were well dispersed in isopropyl alcohol at 6 g L^{-1} without any surfactant and additives. A FTO glass (15 Ω sq.$^{-1}$, Solaronix S.A., Aubonne, Switzerland) was used as the anode during the EPD process by varying the deposition time. The distance between the anode and ITO-PEN was fixed at 1 cm and the applied voltage was kept at 300 V. For the nanocrystalline TiO_2 photoanode film prepared by the EPD process, a mechanical compression (MTS-810, Material Testing System, USA) with different pressures (25–100 MPa) was applied to the film as the post-treatment. The TiO_2 electrodes were immersed in a 3×10^{-4} M solution of N719 (Solaronix S.A., Aubonne, Switzerland) in acetonitrile and tert-butyl alcohol (volume ratio of 1:1) at 40 °C for 3.5 h. The electrodes were separated by a 25 μm-thick Surlyn (SX1170-25, Solaronix S.A., Aubonne, Switzerland) and the working area of the photoanodes was confined by a mask (0.55 cm in diameter). The thick PEDOT film was electropolymerized from the solution that contained 0.1 M $LiClO_4$ and 0.2 M monomer in the ACN solvent. A three-electrode system with a potentiostat (PGSTAT 30, Autolab, Eco-Chemie, the Netherlands) was used. Subsequently, a Pt-sputered (*ca.* 100 nm thick) glass substrate of 0.25 cm^2 active area was applied by a constant potential of 1.0 V (vs. Ag/AgCl (sat'd)) and the passed charge was kept at 60 C cm^{-2}. The supercapacitor was composed of two prepared electrodes of PEDOT film with a working area of 0.25 cm^2, which was put symmetrically face-to-face with an electrolyte of 0.5 M $LiClO_4$ in MPN. The photo-supercapacitor was assembled with a TiO_2 photoanode compressed at 100 MPa, a Pt-sputtered glass and a PEDOT film as shown in Fig. 1, which is a three-electrode liquid type configuration that contained a DSSC and a supercapacitor sharing a common Pt electrode. For the DSSC part, we used Surlyn to separate the counter electrode from the photoelectrode. After injecting the electrolyte, a hot-melt adhe-

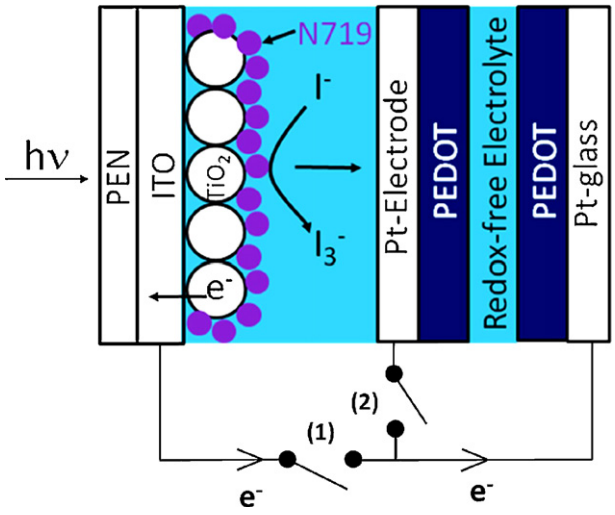

Fig. 1. The configuration of the three-electrode type photo-supercapacitor device which contains a dye-sensitized solar cell and a polymer-based PEDOT supercapacitor sharing a common Pt electrode. For photocharging: (1) and (2) are closed. For discharging: (1) is open and (2) is closed.

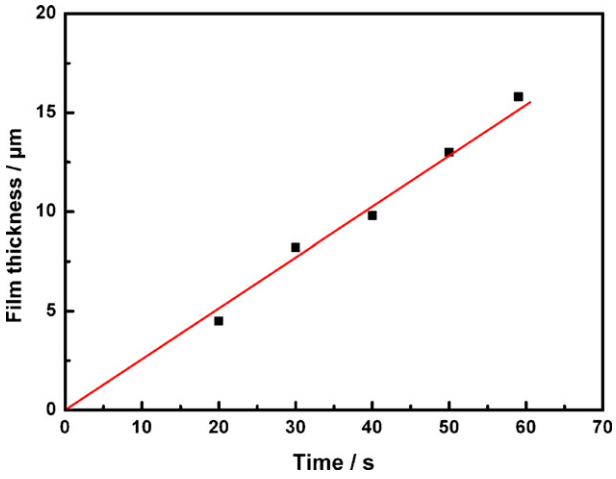

Fig. 2. The linearity of the TiO_2 film thickness vs. the deposition time.

sive was applied to seal the hole. As for the supercapacitor part, we used a double-layer polyimide adhesive as the spacer in the supercapacitor.

2.3. Instrumentation

The photo-supercapacitor and DSSCs were tested by a class A quality solar simulator (PEC-L11, AM1.5G, Peccell Technologies, Inc.) and the incident light intensity of 100 mW cm^{-2} was calibrated with a standard Si Cell (PECSI01, Peccell Technologies, Inc.). Photoelectrochemical behavior and electrochemical impedance spectra (EIS) of the cells were investigated using a potentiostat/galvanostat (PGSTAT 30, Autolab, Eco-Chemie, the Netherlands) under 100 mW cm^{-2} light intensity and the frequency range explored was 10 mHz to 65 kHz. The impedance spectra were analyzed by an equivalent circuit model interpreting the characteristics of the DSSCs [26,27]. The photovoltage transients of DSSCs were recorded with a digital oscilloscope (24×s 200 MHz Oscilloscope, LeCroy), and pulsed laser excitation was applied by a frequency-doubled Q-switched Nd:YAG laser (Spectra-Physics laser, model Quanta-Ray GCR-3-10) with 1 Hz repetition rate at 532 nm and 7 ns pulse width at half-height. The XRD pattern of the TiO_2 powder was analyzed by Rigaku Ultimate IV X-ray diffraction system. Moreover, the film thickness was determined using a surface profilometer (Sloan Dektak 3030) and the morphologies of the film was observed by SEM (NovaTM NanoSEM 230).

3. Results and discussion

3.1. The TiO_2 photoanode prepared by EPD

The realization for the proposed flexible photo-supercapacitor lies in making a reliable flexible TiO_2 photoanode as well as a PEDOT-based supercapacitor. In fact, the former is more important than the latter from a practical point of view. The commercial nanocrystalline TiO_2 particles (P25, 25 nm, 75% anatase and 25% rutile, Degussa) were well dispersed in isopropyl alcohol at 6.0 g L^{-1} without any surfactant or additives. With this dilute and binder-free suspension, one hardly could make a homogeneous TiO_2 film by the doctor-blade process. For this reason, we do not report on the photovoltaic performances of electrodes processed from the same colloidal TiO_2 suspensions using only a compression post-treatment. Besides, a simple compression probably would not be sufficient to get an efficient flexible DSSC. To get a high cell efficiency, one needs to employ both EPD and compression methods. The thickness of the as-deposited TiO_2 nanocrystalline films, prepared by using EPD process was dependent on the deposition time. Other deposition parameters such as the applied voltage, the distance between the electrodes, and the TiO_2 concentration of the EPD solution were fixed and only the deposition time was changed. Our results revealed that under a voltage of 300 V and the TiO_2 solution at a concentration of 6.0 g L^{-1} we obtained a linear relationship between the TiO_2 film thickness and the EPD time as shown in Fig. 2. After the EPD process, the residual IPA solvent on the films was allowed to evaporate for a couple seconds in air at ambient temperature. The as-deposited mesoporous film strongly scattered the light with poor intrinsic mechanical stability, and the film could be easily harmed by scratching. The SEM reveals that the as-deposited TiO_2 film apparently has an obvious crack-rich morphology before post-treatment, as shown in Fig. 3(a). It should be emphasized that although the mesoporous film was crack-rich, the adherence to the ITO-PEN substrate was great enough to be handled easily without exfoliation during the post-treatment. The compression method was employed as a post-treatment in attempt to increase the TiO_2 nanocrystalline interparticles connection. The morphologies of the films were significantly altered after the employment of the mechanical compression as shown in Fig. 3(b). Besides, the mesoporous compressed films became more transparent with less light scattering effect. From the SEM we observed that the as-deposited mesoporous TiO_2 films before mechanical compression (Fig. 3(a)) abounded with cracks about 11–23 μm and showed extremely rough morphology. When the mechanical compression (100 MPa) was applied for 30 s to the film (Fig. 3(b)), the films were smoothed and evened on the cracks. Besides, the pore size of the compressed nanocrystalline TiO_2 films was relatively smaller and much more homogeneous (Fig. 3(b)) than films prepared by only EPD (Fig. 3(a)). In addition, from the dye-loading test, we discovered that at the same film thickness (~11 μm) the amount of the dye-loading for the as-deposited TiO_2 film (0.38×10^{-7} mol cm^{-2}) is much less than that of the compressed TiO_2 films (1.14×10^{-7} mol cm^{-2}). This is because more particles and much compact structures are expected in the compressed film than those in the as-deposited film formed by the EPD. In addition, we can use the following equation [28] to estimate the pressed film porosity prepared from the EPD process:

$$P_p = \frac{L_p - 0.4L_{np}}{L_p} \quad (1)$$

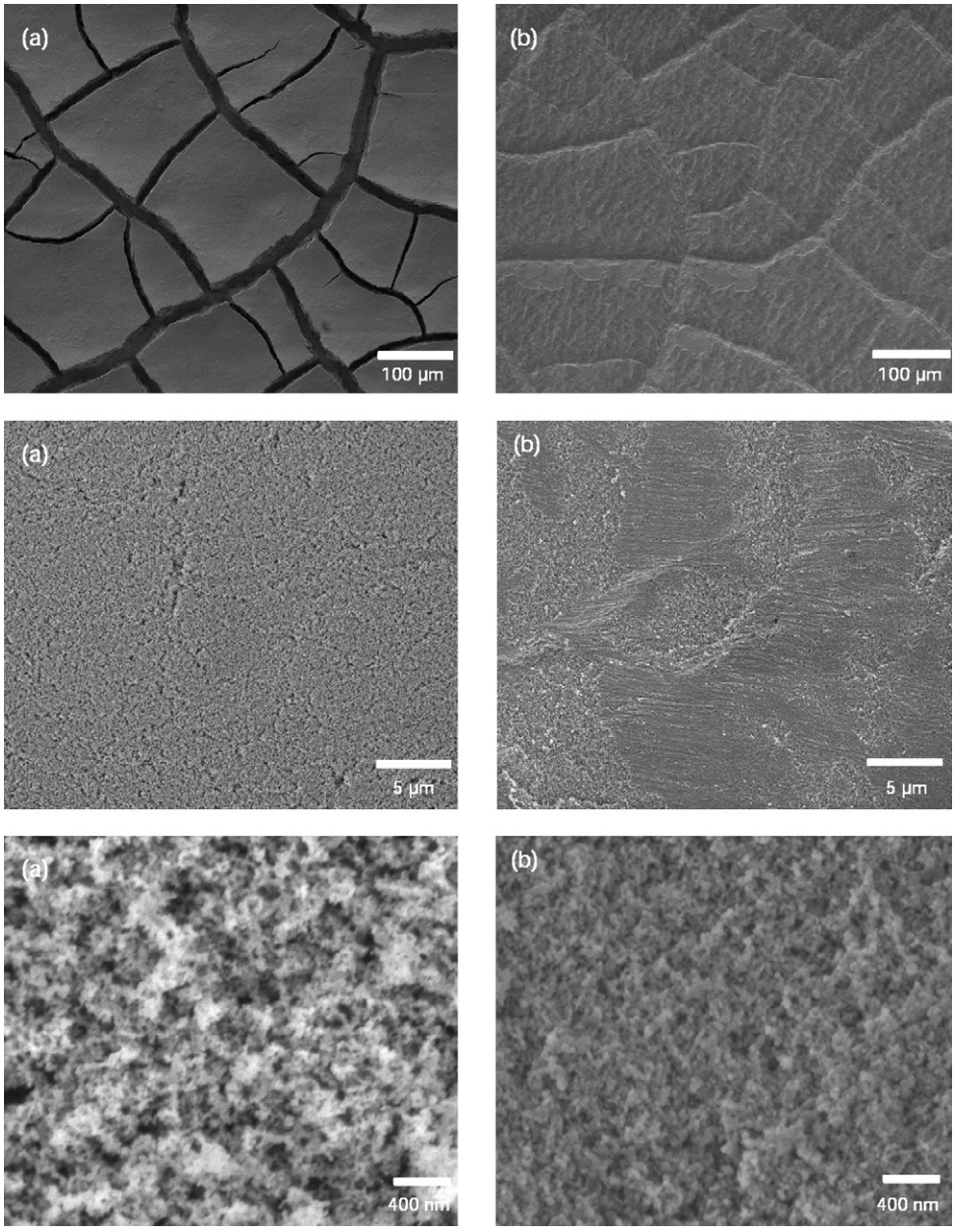

Fig. 3. SEM micrographs (with different magnifications) for the electrophoretically deposited TiO_2 (P25, Degussa) nanostructure (a) as-deposited film, before mechanical compression post-treatment and (b) after mechanical compression post-treatment on the ITO-PEN substrate.

where P_p is the porosity of the pressed film, L_p and L_{np} are the thicknesses of the pressed and unpressed film, respectively. The calculated porosities for various pressed films are included in Table 1, from which the porosity decreasing from 0.56 to 0.42 are noticed. The compression only affects the value of J_{sc}, but not V_{oc}, as the latter remains unchanged. This is because at small porosity, more TiO_2 particles exist in the porous thin film, thus contributing to more dye absorption and electron transfer [29]. As for the adherent test, we used a HB pencil to write on the compressed TiO_2 photoanode and bended the film. It was totally unharmed with extremely great adherence and no peeling off as shown in Fig. 4. Consequently, from these images and data we can observe that the mesoporous TiO_2 structure is very homogeneous, well adherent and without cracks of other defects after the mechanical compression post-treatment.

Table 1
The cell performance and electron lifetimes of DSSCs (measured under 100 mW cm^{-2}) based on TiO_2 films (11 μm) compressed at different pressures during the preparation. Table 1 also includes the estimated values of the porosity (P_p) and the coordination number (N) for all pressed films.

Pressure (MPa)	V_{oc} (V)	J_{SC} (mA cm^{-2})	FF	η (%)	P_p	N	τ_e (ms)	R_{Ct1} (Ω)	R_{Ct2} (Ω)
None	0.77	4.95	0.65	2.36	–	–	–	54.3	33.9
25	0.75	5.56	0.71	2.96	0.56	4.37	1.47	4.2	24.3
50	0.72	7.53	0.71	3.86	0.50	5.03	1.75	4.0	20.8
75	0.74	7.62	0.70	3.94	0.45	5.71	1.82	3.4	20.1
100	0.74	8.38	0.71	4.37	0.42	6.20	2.80	3.2	17.4

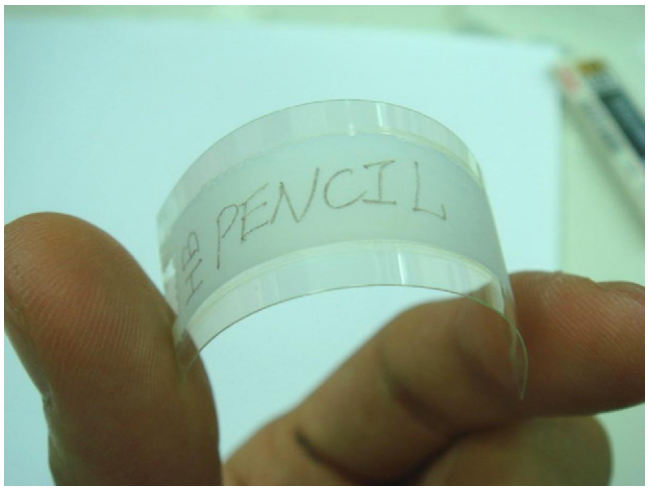

Fig. 4. Image of a bent TiO_2 film compressed at 100 MPa on ITO-PEN substrate with HB pencil writing.

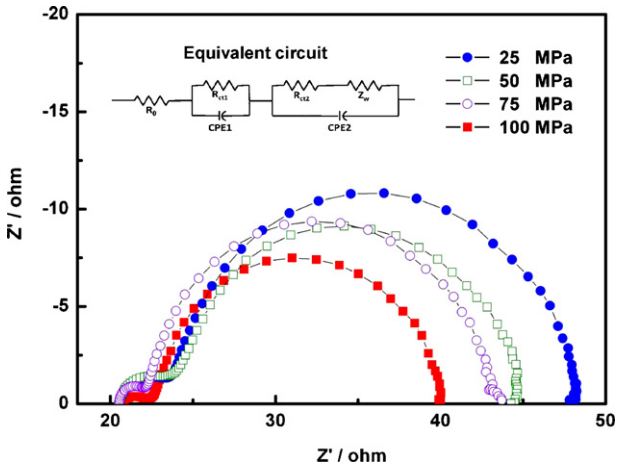

Fig. 6. Electrochemical impedance spectra of DSSCs (under 100 mW cm^{-2}) with films of 11 μm compressed at different pressures.

3.2. The effect of compression on the performance of DSSCs

In order to optimize the pressure for the as-deposited film, the compressed mesoporous TiO_2 film prepared under different pressures were investigated. For the static mechanical compression post-treatment, it not only increases the TiO_2 interparticles connection but also increases the adherence between the nanocrystalline TiO_2 particles and the ITO-PEN substrate that could avoid exfoliation from the substrate. In this work, we tried to prepare the mesoporous TiO_2 film only by the EDP without compressing the film. However, the as-deposited TiO_2 film such prepared had very weak interparticles connection, thus loose mechanical strength. This explains the low photoconversion efficiency.

The *J–V* characteristics of a mesoporous TiO_2 photoanode (~11 μm) prepared by the EPD with a subsequent compressed post-treatment under different pressures is shown in Fig. 5. The low efficiency of the DSSC using the as-deposited TiO_2 film may be resulted from poor interparticles connection, loose adherence to the ITO-PEN substrate and less amount of dye molecules adsorbed. As we can see from the *J–V* curve, the open-circuit voltage was barely affected by the subsequent compressed post-treatment and the photoconversion efficiency is highly related to the photocurrent density. If we fixed the film thickness and changed the compression pressure, the J_{sc} of the cell improved because of the higher coordination number and the better interparticles connection, since more nanocrystalline TiO_2 particles were presented under such condition which enables more dye adsorption. Therefore, part of the photocurrent enhancement is contributed from an increase in the amount of adsorbed Ru complex dye (N719) molecules, which was explained earlier. In addition, the fill factor (*FF*) of the compressed TiO_2 film is significantly larger than that of the as-deposited film. This is attributed to the enhancement of the interfacial connection between the nanocrystalline TiO_2 particles and the ITO-PEN substrate.

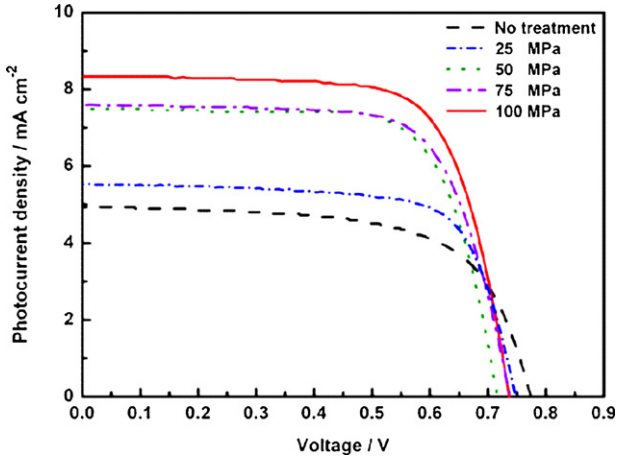

Fig. 5. Photocurrent density vs. voltage characteristics of DSSCs on the ITO-PEN substrate (under 100 mW cm^{-2}) with films of 11 μm compressed at different pressures.

Furthermore, the electrochemical impedance spectroscopy was used to study the internal resistances and the charge-transfer kinetics of the mesoporous TiO_2 films in DSSCs. Fig. 6 shows the Nyquist plots of the EIS of the DSSCs (under 100 mW cm^{-2}) for the compressed TiO_2 film under different pressures at the same film thickness (11 μm). The impedance spectra can be interpreted and modeled using the equivalent circuits proposed in the inset of Fig. 6. Generally, all the impedance spectra of DSSCs contains three semicircles, which are assigned to the electrochemical reaction at the Pt-counter electrode (R_{Ct1}), charge-transfer resistances at the TiO_2/dye/electrolyte interface (R_{Ct2}) and the Warburg diffusion process of I^-/I_3^- in the electrolyte (R_{diff}). In this work, we used a very thin spacer in the device, therefore, the R_{diff} is not obvious and overlapped by R_{Ct2}. The corresponding values of R_{Ct1} and R_{Ct2} are shown in Table 1. The R_{Ct2} decreased as the compressed pressure varied from 25 to 100 MPa, which is also observed in Fig. 6. This phenomenon is related to the increase in the packing density so that the amount of dye adsorption increases in the film as well as the improvement on the adherence at the TiO_2/ITO-PEN interface. On the other hand, the decreased pore size enhances the nanocrystalline TiO_2 interparticles connection, so that the charge-transfer resistance R_{Ct2} decreased as the compressed pressure increased. From the results, it is found that the mesoporous TiO_2 compressed film prepared at 100 MPa not only have a lower charge-transfer resistance but is also expected to have a longer electron lifetime within the TiO_2 photoanode.

Generally, the average electron lifetime can approximately be estimated by fitting a decay of the open-circuit voltage transient with $\exp(-t/\tau_e)$, where t is the time and τ_e is an average time constant before recombination. The effect of pressure for the compressed films on the average electron lifetime was studied by the laser-induced photovoltage transient technique. The data are shown in Fig. 7. From the data, we observed that the electron lifetimes (τ_e) in the compressed mesoporous TiO_2 films were enhanced from 1.47 to 2.80 ms when the compressed pressure increased

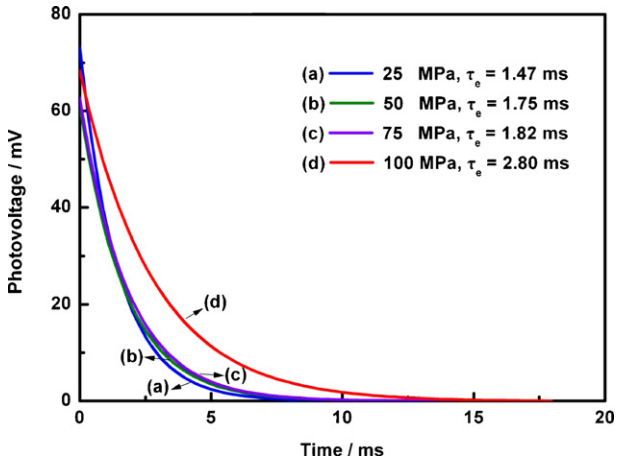

Fig. 7. Transient photovoltage measurements of various TiO_2 photoanodes prepared by compression post-treatment under different pressures.

from 25 to 100 MPa. It implied that the collection and transport of electrons in the TiO_2 film was fastest for the film compressed at 100 MPa. The order of magnitude for τ_e is consistent with the data reported in literature [30]. The XRD patterns of the P25 powder, the as-deposited film, and the film after the compression treatment are shown in Fig. 8. As we can see from the result, the phase compositions of the film before and after the compression are quite similar. Therefore, the compression process does not change the crystallinity of the TiO_2. Moreover, we can use the following equation to estimate the coordination number [31]:

$$N = \frac{3.08}{P_p} - 1.13 \quad (2)$$

where N is the coordination number. The corresponding properties of the mesoporous TiO_2 films compressed at different pressures are listed in Table 1. From the perspective of the electron transport, higher coordination number implies that an electron residing on a particular particle will have more paths by which it can move to an adjoining particle. Therefore, the electron will have better diffusion property in the porous film network leading to better electron lifetime.

As for the thickness effect on the performance of DSSC at the best compressed pressure (100 MPa), the photovoltaic characteristic such as J_{sc}, V_{oc}, FF and η are summarized in Table 2. It can be seen from Fig. 9, the mesoporous TiO_2 film with a thickness of around 11 μm achieved the best cell efficiency of 4.37%, FF of 0.71,

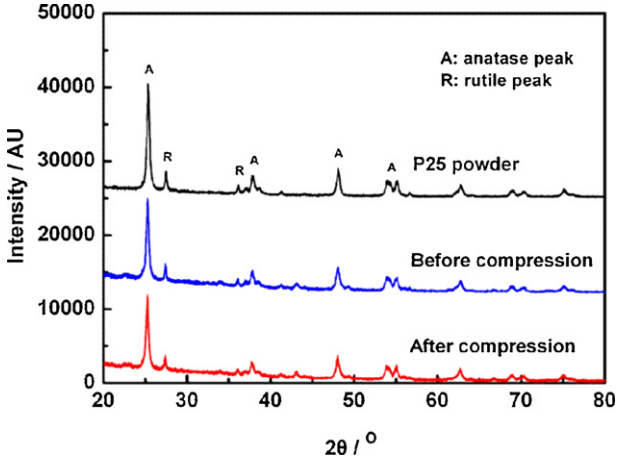

Fig. 8. The XRD patterns of the P25 powder, the film before and after the compression.

Table 2
The cell performance of DSSCs (measured under 100 mW cm^{-2}) based on different thicknesses of TiO_2 photoanode.

Thickness of TiO_2 (μm)	V_{oc} (V)	J_{SC} (mA cm^{-2})	FF	η (%)
6.4	0.73	6.36	0.72	3.37
7.5	0.73	7.24	0.70	3.74
8.4	0.74	7.41	0.70	3.81
10.9	0.74	8.38	0.71	4.37
12.1	0.75	7.70	0.70	4.00

V_{oc} of 0.74 V and J_{sc} of 8.38 mA cm^{-2}. If the film thickness is further increased, it will lower the J_{sc}, FF and η. Although the increase in film thickness tends to raise the amount of dye adsorption, the corresponding higher electron transfer resistance and higher frequency of recombination of electron with I_3^- on the TiO_2 surface leads to smaller V_{oc} and η.

3.3. The performance of the photo-supercapacitor

We combined the components of the previous plastic-based DSSCs (best cell efficiency of 4.37%, FF of 0.71, V_{oc} of 0.74 V and J_{sc} of 8.38 mA cm^{-2}) with a thick PEDOT film, as the electrode material for a bare supercapacitor. The photo-supercapacitor device consists of three electrodes (see Fig. 1), one internal electrode was set as counter electrode and two outer electrodes were connected together as working electrode. The photogenerated electrons flow from the DSSC to the supercapacitor, and the electrons were stored within the conducting PEDOT polymer film. Therefore, the photovoltage was also generated from the TiO_2 photoanode of the DSSC part, which determined the maximum charging voltage of the supercapacitor. The whole device was connected to the potentiostat at the beginning with no current and no voltage responses around 0 V in the dark, as shown in Fig. 10. This implies that the DSSC part would not produce dark current. Subsequently, the photo-supercapacitor was charged by illumination under 100 mW cm^{-2} for 900 s in the short-circuit condition. The photovoltage was rapidly increased and reached a maximum value of 0.69 V which was determined from the photovoltage of the DSSC after illumination for 80 s. After charging for 900 s, the charged photo-supercapacitor was disconnected with the DSSC part left in the open-circuit and remained in the dark for a rest time of 100 s. The charged-state voltage of the photo-supercapacitor decreased gradually and a small drop in the onset voltage of the discharge was noticed, indicating the occurrence of the self-discharge and the existence of the internal resistance of the capacitor [25,32]. Afterward, the photo-supercapacitor was discharged galvanostatically to 0 V at 2 mA cm^{-2} for *ca.* 150 s to return to 0 V as shown in Fig. 10.

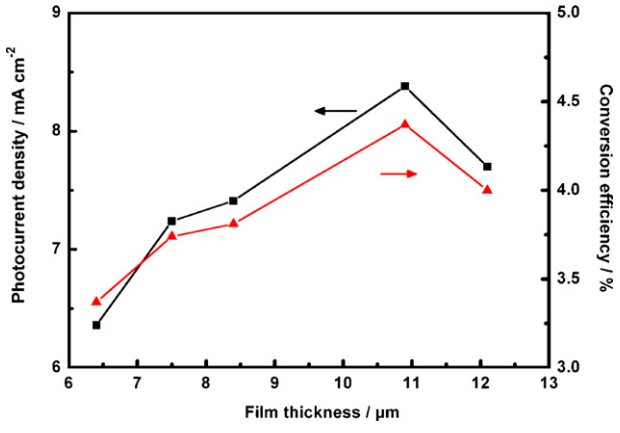

Fig. 9. The photocurrent density and the conversion efficiency using different thickness of TiO_2 photoanode.

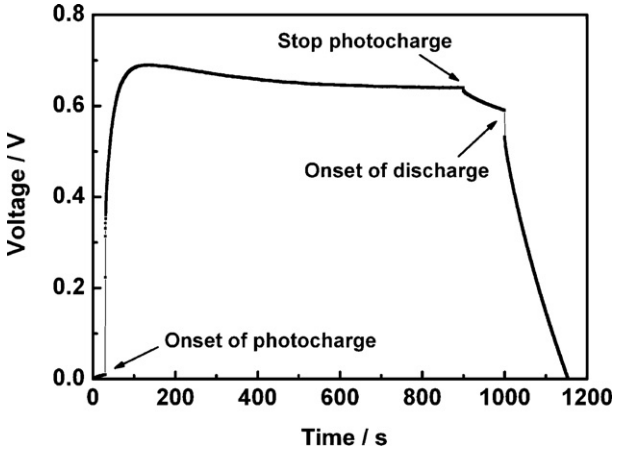

Fig. 10. The dynamic voltage for the photo-supercapacitor under light illumination (under 100 mW cm^{-2}) during charging and discharging processes.

The internal resistance can be calculated from Eq. (3)

$$\Delta V = iR \tag{3}$$

where i is 2 mA cm^{-2} (working area is 0.25 cm^2) and ΔV is about 0.058 V. The internal resistance is estimated to be 160 Ω, which is about half that of the carbon-based photocapacitor [25]. This is because we employed a PEDOT conducting polymer electrode in the supercapacitor, which has a high surface area and high conductivity, thus leading to a lower internal resistance.

In addition, we can obtain the specific capacitance of the photo-supercapacitor from the charging voltage and the time by Eq. (1) [33] to be 0.52 F cm^{-2}

$$C = \frac{i}{\Delta V/\Delta t} \tag{4}$$

where C is the specific capacitance in F, i is the charge/discharge current in A, $\Delta V/\Delta t$ is the voltage change per time in V s^{-1}. Further research on the cycle-life, the tolerance to overcharge, as well as other related issues is under way.

4. Conclusions

We propose a novel flexible photo-supercapacitor using PEDOT thick film and dye N719-TiO_2 photoactive layer for dual application on solar cell and energy storage. For the plastic-based DSSC part, the best performance (cell efficiency of 4.37%, *FF* of 0.71, V_{oc} of 0.74 V and J_{sc} of 8.38 mA cm^{-2}) was achieved with a 11 μm TiO_2 photoanode after compressing at 100 MPa. Besides, the R_{Ct2} of 17.4 Ω and the dye-loading amount of 1.14×10^{-7} mol cm^{-2} for the compressed TiO_2 film under 100 MPa with a thickness of 11 μm can be also observed. In addition, for the photo-supercapacitor the thick PEDOT film is electropolymerized to *ca.* 0.5 mm combined with plastic-based DSSC and the specific capacitance of 0.52 F cm^{-2} has been reached. The mesoporous TiO_2 film was prepared by the EPD on plastic ITO-PEN substrate following a compression post-treatment to enhance the interparticles connection among nanocrystalline TiO_2 and to improve the adherence on the ITO-PEN plastic substrate. The major task of fabricating a flexible photo-supercapacitor can be regarded as the photoelectrode part; therefore, improving the performance of the plastic-based flexible photoelectrode is important. As long as the photoelectrode can achieve high performance and fabricated well on the flexible substrate then it is applicable to all plastic-based photo-supercapacitor device. This study shows a promising technique for application on either DSSC or photo-supercapacitor.

Acknowledgements

This work was financially sponsored by a grant from the National Taiwan University. Some of the instruments used in this study were made available through the support of the National Science Council (NSC) of Taiwan.

References

[1] M. Grätzel, J. Photochem. Photobiol. A: Chem. 164 (2004) 3–18.
[2] A. Hagfeldt, M. Grätzel, Acc. Chem. Res. 33 (2000) 269–277.
[3] A. Kay, M. Grätzel, Sol. Energy Mater. Sol. Cells 44 (1996) 99–117.
[4] M.K. Nazeeruddin, R. Humphry-Baker, P. Liska, M. Grätzel, J. Phys. Chem. B 107 (2003) 8981–8987.
[5] M.K. Nazeeruddin, F.D. Angelis, S. Fantacci, A. Selloni, G. Viscardi, P. Liska, S. Ito, B. Takeru, M. Grätzel, J. Am. Chem. Soc. 127 (2005) 16835–16847.
[6] F. Gao, Y. Wang, D. Shi, J. Zhang, M. Wang, X. Jing, R.H. Baker, P. Wang, S.M. Zakeeruddin, M. Grätzel, J. Am. Chem. Soc. 130 (2008) 10720–10728.
[7] N.G. Park, K.M. Kim, M.G. Kang, K.S. Ryu, S.H. Chang, Y.J. Shin, Adv. Mater. 17 (2005) 2349–2353.
[8] T. Miyasaka, M. Ikegami, Y. Kijitori, J. Electrochem. Soc. 154 (2007) A455–A461.
[9] Y. Kijitori, M. Ikegami, T. Miyasaka, Chem. Lett. 36 (2007) 190–191.
[10] Z. Tebby, O. Babot, D. Michau, L. Hirsch, L. Carlos, T. Toupanc, J. Photochem. Photobiol. A 205 (2009) 70–76.
[11] S. Uchida, M. Tomiha, N. Masaki, A. Miyazawa, H. Takizawa, Sol. Energy Mater. Sol. Cells 81 (2004) 135–139.
[12] H.C. Weerasinghe, P.M. Sirimanne, G.P. Simon, Y.B. Cheng, J. Photochem. Photobiol. A 206 (2009) 64–70.
[13] A.D. Pasquier, M. Stewart, T. Spitler, M. Coleman, Sol. Energy Mater. Sol. Cells 93 (2009) 528–535.
[14] T. Miyasaka, Y. Kijitori, J. Electrochem. Soc. 151 (2004) A1767–A1773.
[15] H. Lindström, A. Holmberg, E. Magnusson, L. Malmqvist, A. Hagfeldt, J. Photochem. Photobiol. A 145 (2001) 107–112.
[16] H. Lindström, A. Holmberg, E. Magnusson, S.E. Lindquist, L. Malmqvist, A. Hagfeldt, Nano Lett. 1 (2001) 97–100.
[17] G. Boschloo, H. Lindström, E. Magnusson, A. Holmberg, A. Hagfeldt, J. Photochem. Photobiol. A 148 (2002) 11–15.
[18] J.H. Yum, S.S. Kim, D.Y. Kim, Y.E. Sung, J. Photochem. Photobiol. A 173 (2005) 1–6.
[19] L. Grinis, S. Dor, A. Ofir, A. Zaban, J. Photochem. Photobiol. A 198 (2008) 52–59.
[20] L. Grinis, S. Kotlyar, S. Rühle, J. Grinblat, A. Zaban, Adv. Funct. Mater. 19 (2009) 1–7.
[21] M. Dürr, A. Schmid, M. Obermaier, S. Rosselli, A. Yasuda, G. Nelles, Nat. Mater. 4 (2005) 607–611.
[22] T. Yamaguchi, N. Tobe, D. Matsumoto, H. Arakawa, Chem. Commun. (2007) 4767–4769.
[23] G.A. Snook, C. Peng, D.J. Fray, G.Z. Chen, Electrochem. Commun. 9 (2007) 83–88.
[24] T. Miyasaka, T.N. Murakami, Appl. Phys. Lett. 85 (2004) 3932–3934.
[25] T.N. Murakami, N. Kawashima, T. Miyasaka, Chem. Commun. 26 (2005) 3346–3348.
[26] L. Han, N. Koide, Y. Chiba, T. Mitate, Appl. Phys. Lett. 84 (2004) 2433–2435.
[27] L. Han, N. Koide, Y. Chiba, A. Islam, T. Mitate, C.R. Chim. 9 (2006) 645–651.
[28] A. Ofir, T. Dittrich, S. Tirosh, L. Grinis, A. Zaban, J. Appl. Phys. 100 (2006) 0743171–0743176.
[29] M. Ni, M.K.H. Leung, D.Y.C. Leung, K. Sumathy, Sol. Energy Mater. Sol. Cells 90 (2006) 1331–1344.
[30] C.P. Hsu, K.M. Lee, J.T.W. Huang, C.Y. Lin, C.H. Lee, L.P. Wang, S.Y. Tsai, K.C. Ho, Electrochim. Acta 53 (2008) 7514–7522.
[31] J. van de Lagemaat, K.D. Benkstein, A.J. Frank, J. Phys. Chem. B 105 (2001) 12433–12436.
[32] A. Du Pasquier, I. Plitz, J. Gural, S. Menocal, J. Power Sources 113 (2003) 62–71.
[33] J. Tanguy, N. Mermilliod, M. Hoclet, J. Electrochem. Soc. 134 (1987) 795–802.